European Journal of Pharmaceutical Sciences 107 (2017) 112–125

Contents lists available at ScienceDirect

European Journal of Pharmaceutical Sciences

journal homepage: www.elsevier.com/locate/ejps

Macrophage selective photodynamic therapy by meta-tetra(hydroxyphenyl) chlorin loaded polymeric micelles: A possible treatment for cardiovascular diseases

Jos W.H. Wennink[a,1], Yanna Liu[a,1], Petri I. Mäkinen[b], Francesca Setaro[c], Andrès de la Escosura[c], Meriem Bourajjaj[a], Jari P. Lappalainen[b], Lari P. Holappa[b], Joep B. van den Dikkenberg[a], Mina al Fartousi[a], Panagiotis N. Trohopoulos[d], Seppo Ylä-Herttuala[b,e], Tomas Torres[c,f,g], Wim E. Hennink[a], Cornelus F. van Nostrum[a,*]

[a] Department of Pharmaceutics, Utrecht Institute for Pharmaceutical Sciences (UIPS), Utrecht University, Universiteitsweg 99, 3508 TB Utrecht, Netherlands
[b] A.I. Virtanen Institute for Molecular Sciences, University of Eastern Finland, Neulaniementie 2, Kuopio FIN-70211, Finland
[c] Departamento de Química Orgánica, Universidad Autónoma de Madrid (UAM), Cantoblanco, 28049 Madrid, Spain
[d] CosmoPHOS Ltd, 77 Tsimiski str., GR-54622 Thessaloniki, Greece
[e] Heart Center and Gene Therapy Unit, Kuopio University Hospital, 70211 Kuopio, Finland
[f] Institute for Advanced Research in Chemical Sciences (IAdChem), UAM, 28049 Madrid, Spain.
[g] Instituto Madrileño de Estudios Avanzados (IMDEA)-Nanociencia c/Faraday, 9, Cantoblanco, 28049 Madrid, Spain

ARTICLE INFO

Keywords:
Polymer micelles
Photodynamic therapy
Atherosclerosis
Drug targeting
Drug release

ABSTRACT

Selective elimination of macrophages by photodynamic therapy (PDT) is a new and promising therapeutic modality for the reduction of atherosclerotic plaques. m-Tetra(hydroxyphenyl)chlorin (mTHPC, or Temoporfin) may be suitable as photosensitizer for this application, as it is currently used in the clinic for cancer PDT. In the present study, mTHPC was encapsulated in polymeric micelles based on benzyl-poly(ε-caprolactone)-*b*-methoxy poly(ethylene glycol) (Ben-PCL-mPEG) using a film hydration method, with loading capacity of 17%. Because of higher lipase activity in RAW264.7 macrophages than in C166 endothelial cells, the former cells degraded the polymers faster, resulting in faster photosensitizer release and higher in vitro photocytotoxicity of mTHPC-loaded micelles in those macrophages. However, we observed release of mTHPC from the micelles in 30 min in blood plasma in vitro which explains the observed similar in vivo pharmacokinetics of the mTHPC micellar formulation and free mTHPC. Therefore, we could not translate the beneficial macrophage selectivity from in vitro to in vivo. Nevertheless, we observed accumulation of mTHPC in atherosclerotic lesions of mice aorta's which is probably the result of binding to lipoproteins upon release from the micelles. Therefore, future experiments will be dedicated to increase the stability and thus allow accumulation of intact mTHPC-loaded Ben-PCL-mPEG micelles to macrophages of atherosclerotic lesions.

1. Introduction

At present the world population encounters increase in age, obesity and lack of physical activity (Roger et al., 2012). This can give imbalance in the human physiology leading to among others high blood pressure, diabetes and unhealthy cholesterol levels, which eventually cause cardiovascular diseases being the number one cause of death in the western world. The prevalent contributor to cardiovascular morbidity is atherosclerosis, a chronic inflammation with slow progressive buildup of lipids and macrophages within the arterial wall (Libby et al., 2002). Lipid build up can start in the early thirties of a human's life and cause signs and symptoms 20 years later. Atherosclerosis is the main cause of myocardial infarctions and atherosclerotic plaque rupture.

When atherosclerosis is detected in an early phase, administration of hypolipidemic agents has mostly been applied as a therapy for the last two decades (Gotto and Pownall, 2015). More recently, novel therapeutic strategies involving treating vessel wall inflammation have emerged (Tabas and Glass, 2013). However, after administration of anti-inflammatory drugs there is a chance on the occurrence of side effects, primarily systemic immunosuppression and other off target

* Corresponding author.
E-mail address: C.F.vannostrum@uu.nl (C.F. van Nostrum).
[1] Both authors contributed equally to this paper.

http://dx.doi.org/10.1016/j.ejps.2017.06.038
Received 7 December 2016; Received in revised form 1 June 2017; Accepted 30 June 2017
Available online 02 July 2017

effects (John and Kitas, 2012). When atherosclerosis is detected in a later phase it is mainly due to myocardial infarctions. In this stage the options are more rigorous and are mainly focused on opening the vessel by balloon angioplasty (Gray and Sullivan, 1996) with or without stenting (Farb et al., 1999) and in the most severe cases a bypass vessel (Sarjeant and Rabinovitch, 2002) will be installed. Currently much research is directed to repairing affected vessels by tissue engineered vessels that lack the drawbacks (unfavorable compliance and high stiffness) of current bypass vessels (Song et al., 2011a, 2011b). Until now none of these methods are actually treating or removing the inflammation and reoccurrence of myocardial infarctions in atherosclerotic patients is high (Davidsen et al., 2002; Smolina et al., 2012).

A new and promising combination therapy for the treatment of atherosclerotic plaques is photodynamic therapy (PDT) (Drakopoulou et al., 2011). A pivotal component of PDT in promoting plaque stabilization is sustained macrophage removal. Waksman et al. showed that PDT can reduce plaque formation and promotes smooth muscle cell repopulation if the macrophages are properly targeted (Waksman et al., 2008). Photodynamic therapy (PDT) is based on three interacting elements: 1) a non-aggregated photosensitizer (PS); 2) light of appropriate wavelength to activate the PS and 3) tissue oxygen (Henderson and Dougherty, 1992). When the PS is activated by light to the excited state and returns to the ground state, it releases energy, which is transferred to the surrounding tissue oxygen to generate singlet oxygen which in turn causes cell death (Guo et al., 2010). However, aggregation of PS molecules must be prevented, since the quantum yield of PS emission is highly dependent on its aggregation state (Ozoemena et al., 2001). Selective exposure of the plaque regions by light can be accomplished using an intra-arterial light emitting catheter (Jenkins et al., 1999). However, illumination of endothelial cell lining of the arteries that have possibly taken up PS can lead to atherosclerotic plaque rupture (Demidova and Hamblin, 2004), which should by all means be avoided. Therefore, selectively targeting the neo-vessels inside the plaques and/or the macrophages located in the plaques is highly desired. Importantly, most effective PS have low water solubility, therefore a simple intravenous injection is complicated and a safe solubilizing excipient or carrier system is necessary.

If one aims for PDT to become the future treatment of atherosclerosis, the problems stated above have to be overcome (Mulder et al., 2014). A method to circumvent these problems is by encapsulating the hydrophobic PS in nanoparticles. Besides enabling intravenous injection, nanoparticles are also known for enhancing therapeutic efficacy and safety of encapsulated drugs by improving solubility, ability of combining multiple drugs, protecting against metabolism, and controlling release (Mulder et al., 2014; Szelenyi, 2012). Furthermore, the formation of leaky vessels from the vasa vasorum in atherosclerotic plaques allows for accumulation of nanoparticles by the enhanced permeability and retention (EPR) effect inside the plaque and avoids uptake by the endothelium layer (Fang et al., 2011). Current research in atherosclerosis and nanoparticles primarily focuses on the targeted delivery of anti-inflammatory drugs (Lobatto et al., 2015; Sanchez-Gaytan et al., 2015; van der Valk et al., 2015), however such drugs usually only delay progression of atherosclerosis (Berman et al., 2013) thereby becoming a reoccurring medication during the lifetime of patients. In the present study we therefore combine the advantages of PDT and nanomedicine to develop a curative treatment for atherosclerosis.

Meta-tetra(hydroxyphenyl)chlorine (mTHPC) is a photosensitizer currently used in the PDT treatment of squamous-cell carcinoma (Lorenz and Maier, 2008) and available in a variety of commercial and EMA approved formulations including liposomes (Foscan®, FosLip®, FosPEG®). Previous research in our group showed that benzyl-functionalized micelles based on poly(ε-caprolactone)-*b*-methoxy poly(ethylene glycol) (Ben-PCL-mPEG) block copolymers can encapsulate mTHPC with very high loadings and remarkable stability (Carstens et al., 2007, 2008; Hofman et al., 2008). Most interestingly, it was shown that the release and subsequent photocytotoxic activity of mTHPC are controlled by lipase induced enzymatic degradation of the micelles (Hofman et al., 2008). This can be advantageous since it is known that macrophages present in the plaque synthesize lipoprotein lipase (LPL) (O'Brien et al., 1992), and therefore we hypothesized that it could thus potentially promote local release and activation of the photosensitizer once the loaded micelles are delivered to and internalized by the macrophages.

In this paper, mTHPC-loaded micelles were conveniently prepared by a film hydration method. We investigated if the LPL produced in macrophages can provide some cell specificity as compared to endothelial cells due to the enzymatic degradation of the micelles. The small size of the micelles might be advantageous for plaque penetration by the EPR effect. However, to selectively deliver the micelles to macrophages in the plaques, the micelles should at least be stable and retain their cargo during circulation. Therefore, we evaluated the in vitro stability in blood plasma and the in vivo pharmacokinetics of the mTHPC-loaded Ben-PCL-mPEG micelles.

2. Materials and methods

2.1. Materials

Acetonitrile, dimethyl sulfoxide (DMSO), trifluoroacetic acid, hydrogen peroxide, fetal bovine serum (FBS), trypsin, EDTA, PBS, ethanol, propylene glycol and high glucose Dulbecco modified eagle medium (DMEM) were obtained from Sigma-Aldrich (Zwijndrecht, the Netherlands). 384-Well plates were purchased from Fisher scientific GmbH (German). Optimem phenol red free was purchased at Invitrogen (Bleiswijk, the Netherlands). CellTiter 96® AQ_{ueous} One Solution was obtained from Promega (Leiden, the Netherlands). Human plasma and mice plasma were purchased from Seralab (UK) and mTHPC was purchased from Molekula (Germany). Foslip® (mTHPC liposomal formulation) and Foscan® (mTHPC in ethanol:propylene glycol 40/60 w/w) was kindly provided by Biolitec AG (Jena, Germany). Foslip® is composed of Phospholipids, glucose, and mTHPC with a dye: lipid ratio of ca. 1:13. Foslip® was reconstituted from lyophilized powder in distilled water. Foscan diluent is referred to a mixture of ethanol: propylene glycol (40/60 w/w).

2.2. Micelle formation

Micelles with and without mTHPC loading were formed by the film hydration method (Carstens et al., 2007). In short, 10 mg of Ben–PCL-mPEG block copolymer was dissolved in 1 mL of dichloromethane. Next, 5 mg of mTHPC was dissolved in 1 mL THF and different amounts corresponding to the desired polymer/photosensitizer ratios were mixed with the dichloromethane block copolymer solution. After evaporation of dichloromethane and THF in a vacuum oven, a thin solid film was formed. The formed film contained both block copolymers and photosensitizer that was visually distributed in a homogeneous way. The block copolymer (+ photosensitizer) film was subsequently hydrated in 1 mL PBS solution by gentle shaking and after 1 h subsequently filtered through a 0.2 μm syringe filter to remove non-encapsulated and thus precipitated photosensitizer. This procedure results in empty micelles or photosensitizer loaded micellar dispersions of 10 mg/mL Ben-PCL_n-$mPEG_{45}$. Size of micelles (by DLS) and critical micelle concentration were determined as described in Supplementary material.

2.3. Loading efficiency and capacity of micelles

The concentration of mTHPC in micellar dispersions was determined by UV/Vis spectroscopy. The dispersions were diluted in DMF to dissolve the micelles. A spectrum between 300 and 800 nm was recorded by a Shimadzu UV-2450 spectrophotometer (Shimadzu, Japan). The absorbance at 650 nm was analyzed against a calibration curve of

mTHPC in DMF, which was linear between 0.1 and 6 μg/mL. The loading efficiency and loading capacity were calculated by Eqs. (1) and (2), respectively.

$$LE\ (\%) = \frac{mTHPC\ loaded\ (mg)}{mTHPC\ fed\ (mg)} \times 100\% \quad (1)$$

$$LC\ (\%) = \frac{mTHPC\ loaded\ (mg)}{polymer\ \ used\ (mg) + mTHPC\ loaded\ (mg)} \times 100\% \quad (2)$$

2.4. Aggregation state of mTHPC

Absorption spectra were measured to determine the aggregation state of the mTHPC in the polymeric micelles. mTHPC loaded micelles were 20 fold diluted in PBS and analyzed with UV/Vis spectrophotometry (Shimadzu UV-2450 spectrophotometer) from 300 to 800 nm. The recorded samples were compared to free mTHPC dissolved in DMF. If the mTHPC aggregates, the 650 nm peak shows a distinctive red or blue shift.

2.5. Singlet oxygen production of mTHPC loaded micelles

$^1O_2$ quantum yields (Φ_Δ) were measured in DMSO (for the non-encapsulated mTHPC) and D_2O (for the mTHPC-loaded micelles), following the *relative method*, based on the photoinduced decomposition of a chemical (i.e., 1,3-diphenylisobenzofuran (DPBF) in DMSO, and α,α'-(anthracene-9,10-diyl)bimethylmalonate (ADMA) in D_2O) that reacts readily with $^1O_2$ (Makhseed et al., 2012; Nombona et al., 2012). Non-substituted ZnPc ($\Phi_{\Delta(DMSO)} = 0.67$) (Kuznetsova et al., 2000) and eosin Y ($\Phi_{\Delta(D2O)} = 0.60$) (Ma et al., 2008) were used as the respective reference compounds.

A stock solution of scavenger (DPBF in DMSO or ADMA in D_2O, volume was 2.5 mL with an absorbance of ca. 1) was transferred into a 1 × 1 cm quartz optical cell and flushed with oxygen for 1 min. A concentrated stock solution of the mTHPC (non-encapsulated or loaded in micelles) in the corresponding solvent was then added in a defined amount to reach a final Q-band absorbance value of about 0.1 (λ = 650 nm). The solution was stirred and irradiated for defined time intervals, using a halogen lamp (typically, 300 W). The duration of these intervals is tuned in each experiment, in order to get a decrease in scavenger absorption of about 3–4% per irradiation interval. Incident light was filtered through a water filter (6 cm) and an additional filter to remove light under 455 nm (Newport filter 20CGA-455). The decrease of scavenger concentration with irradiation time was monitored at 414 and 379 nm, respectively. For quantum yield determination, the experiment was performed three times and the obtained data represent mean values of those three experiments. The estimated error is ± 10%. Singlet oxygen quantum yield (Φ_Δ) was calculated using the following equation:

$$\phi_\Delta^S = \phi_\Delta^R \frac{k^S I_{aT}^R}{k^R I_{aT}^S}$$

where k is the slope of a plot of ln (A_0/A_t) versus irradiation time t, with A_0 and A_t being the absorbance of scavenger at the monitoring wavelength before and after irradiation time t, respectively. I_{aT} is the total amount of light absorbed by the dye. Superscripts R and S indicate reference and sample, respectively. I_{aT} is calculated as a sum of intensities of the absorbed light I_a at wavelengths from the filter cutoff to 800 nm (step 0.5 nm). I_a at given wavelength is calculated using Beer's law:

$$I_a = I_0(1 - e^{-2.3A})$$

where transmittance of the filter at a given wavelength stays for I_0 and the absorbance of the dye at this wavelength stays for A.

2.6. Cell culture

2.6.1. RAW264.7 macrophages

Vials of RAW264.7 macrophages (passage 4) were thawed and taken into culture in a T75 flask. The cells were harvested by washing with 12 mL PBS. After washing, 2 mL of PBS was added and a cell scraper was used to detach RAW264.7 macrophages from the T75 flask. Next, 4 mL high glucose (4500 mg/L) DMEM medium containing 10% FBS was added and the cell suspensions were transferred into a sterile 12 mL tube and centrifuged at 200 relative centrifugal force (rcf) for 3 min at 4 °C. The supernatant was discarded and the cells were suspended in 1 mL of the same medium by repeatedly pipetting using a 200 μL pipette to remove cell lumps. Subsequently, 9 mL of the same medium was added to yield a final volume of 10 mL. Accordingly, the cell density and viability were determined by counting the cells with a Burker Turk cell counter after staining with trypan blue.

2.6.2. C166 endothelial cells

Vials of C166 endothelial cells (passage 27) were thawed and taken into culture in a T75 flask. The cells were harvested by washing with 12 mL PBS followed by detaching the cells from the flask with 2 mL of 0.25% (w/v) trypsin/0.53 mM EDTA solution. Next, 4 mL high glucose DMEM medium containing 10% FBS was added and the cell suspensions were transferred into a sterile 12 mL tube and centrifuged at 200 rcf for 3 min at 4 °C. The supernatant was discarded and the cells were re-suspended in 10 mL of the same medium. Finally, the cell density and viability were determined by counting the cells with a Burker Turk cell counter after staining with trypan blue.

2.6.3. Dark toxicity and photocytotoxicity

Cell viability was determined with a CellTiter 96® AQ_{ueous} One Solution (Promega) containing 3-(4,5-dimethylthiazol-2-yl)-5-(3-carboxymethoxyphenyl)-2-(4-sulfophenyl)-2H-tetrazolium (MTS). The MTS is converted by enzymes present in the mitochondria of the living cells to form formazan. The quantity of formazan produced is proportional to the amount of living cells and is detected by measuring absorbance at 490 nm.

In short, 10,000 cells/well murine RAW264.7 macrophages or 4000 cells/well murine endothelial C166 cells were seeded into 96 well plates and incubated overnight in 100 μL high glucose DMEM medium containing 10% FBS per well. After overnight incubation at 37 °C and 5% CO_2 the medium was aspirated and replaced by with 50 μL high glucose DMEM medium containing 10% FBS and 50 μL mTHPC micelles formulations in PBS. The incubation time for the uptake of the mTHPC micelles was varied between 1and 24 h. For dark toxicity, the cells loaded in the wells were kept in the dark for 24 h. For photocytotoxicity experiments, after the chosen incubation time, the cells were illuminated for 10 min with 3.5 mW/cm^2 light intensity, using a homemade device consisting of 96 LED lamps (670 ± 10 nm, 1 LED per well).

To give time for the dead cells to detach from the surface of the wells, the illuminated plate was placed in an incubator for 1 h at 37 °C and 5% CO_2. Next, the medium was aspirated and to each well 100 μL high glucose DMEM medium containing 10% FBS and 20 μL of CellTiter 96® AQ_{ueous} One Solution was added. Subsequently, the well plate was incubated for 4 h at 37 °C and 5% CO_2 and the absorbance at 490 nm was measured with a 96 well plate reader (Biochrom EZ Read 400 Microplate reader, Biochrom, U.K.)

2.7. Colorimetric lipase activity assay

RAW264.7 macrophages or endothelial C166 cells (both 4000 cells/well) were seeded into 96 well plates and incubated overnight in 100 μL high glucose DMEM medium containing 10% FBS for each well at 37 °C and 5% CO_2. The medium was aspirated and the protocol according the colorimetric lipase activity assay kit II from Sigma-Aldrich was used to determine the lipase activity. Hundred μL of Master mix (Sigma

Aldrich, 85 µL lipase assay buffer, 10 µL DTNB and 5 µL lipase substrate) were added to the wells. Subsequently, the plate was placed in a well plate reader (SPECTROstar^{nano}, BMG labtech, Germany) at 37 °C and the absorbance was measured at 412 nm ($A_{412,\ initial}$). Subsequently, every 2 min the absorbance was measured for 30 min or until the values exceeded the TNB calibration curve ($A_{412,\ final}$). The change in absorbance was calculated by subtracting $A_{412,\ initial}$ from $A_{412,\ final}$ and the resulting ΔA_{412} was compared with the absorbance of the TNB calibration curve to determine the amount of TNB produced. The formed amount TNB is proportional to the amount of enzyme present. One unit of lipase is the amount of enzyme that generates 1.0 µmol of TNB per minute at 37 °C. From this the lipase activity was calculated in milliunits/mL (abbreviated as mU/mL).

2.8. Fluorescence microscopy

RAW264.7 macrophages or C166 endothelial cells were seeded in uncoated six channel µ-Slides (µ-slide IV 0.4 ibitreat, Ibidi, Germany) with 20,000 or 8000 cells per channel, respectively. The slides were incubated for 1 h at 37 °C and 5% CO_2 and the medium was refreshed with high glucose DMEM medium containing 10% FBS. After an overnight incubation at 37 °C and 5% CO_2, the medium was refreshed again and replaced with the same medium and the mTHPC formulation (500 µg/mL Ben-PCL_7-$mPEG_{45}$ and 4 µg/mL mTHPC). After incubation times of 1, 2, 4, 8 and 24 h, the slides were washed with PBS. After washing, 150 µL Optimem Phenol red free was added to the cells. The slides were imaged with a Deltavision Elite Microscope equipped with an incubation chamber set at 37 °C and a mCherry filter (λ_{ex} 575/25 nm, λ_{em} 625/36 nm). The exposure time was 600 ms.

2.9. In vitro stability of micelles in serum and blood plasma

The in vitro stability of mTHPC-loaded micelles based on Ben-PCL_7-$mPEG_{45}$ and containing different mTHPC loadings was studied in FBS, mouse plasma and human plasma dilutions with various concentrations of plasma proteins at 37 °C, by monitoring the change of fluorescence intensity of mTHPC using a Jasco FP8300 spectrofluorimeter (Japan). Foslip® (a liposomal formulation of mTHPC) and Foscan® (free mTHPC) were used as reference.

Foscan® with different concentrations of mTHPC was prepared by adding certain amounts of Foscan diluent (ethanol:propylene glycol, 40/60 w/w) to a stock solution of 3 mg/mL Foscan®. mTHPC loaded micelles with different photosensitizer loadings (0.1% to 20% w/w) were prepared in PBS as described in Section 2.2 (polymer concentration was fixed at 10 mg/mL). Foslip® solutions were prepared at different mTHPC concentrations by preparing a 3 mg/mL stock solution in PBS and diluting this with PBS. FBS, human or mouse plasma were diluted in different amounts of PBS to get 10, 50 and 90% serum or plasma solutions. mTHPC samples were added to the different serum/plasma solutions with the ratio of 1:9 (v/v). As controls, samples were mixed with PBS (1:9 v/v). After incubation at 37 °C, samples were taken at different time points (5, 15, 35 min, and 1, 1.5, 2, 3, 4, 6, 8 h) and added in a 384-Well plate. After taking the samples, the fluorescence intensity was recorded using a Jasco FP8300 spectrofluorimeter at 655 nm after excitation at 420 nm. All fluorescence measurements were carried out in duplicate.

2.10. In vivo studies

2.10.1. Pharmacokinetics in healthy mice

All animal experiments were approved by local and national regulatory authorities and by an animal ethics welfare committee. All procedures involving animals were performed under general anesthesia with inhaled isoflurane using a Univentor 400 anesthesia unit (Genestil, Royaucourt, France), with every effort made to minimize suffering.

For in vivo pharmacokinetic study, female Balb/c nude mice of 6–8 weeks age, weighing 16–22 g were purchased from Envigo. Mice were housed in ventilated cages at 25 °C and 55% humidity under natural light/dark conditions and allowed free access to standard food and water. Mice were divided into two groups (n = 3 per group), which were intravenously injected via the tail vein with 100 µL mTHPC loaded micelles in PBS at 5% (w/w) loading (high mTHPC dose) and 0.6% (w/w) loading (low mTHPC dose), respectively (solutions containing 1 mg Ben-PCL_7-$mPEG_{45}$ and 50 µg mTHPC for the high dose group or 6 µg mTHPC in PBS for the low dose group). About 50 µL of blood samples were taken and collected in heparinized tubes at different time points post injection via cheek puncture. Each collected blood sample was centrifuged for 15 min at 1000 × *g* at 4 °C. Afterwards, the clear supernatant was collected and vortex-mixed with acetonitrile: DMSO (4:1 v/v) for 1 min. The mixture was centrifuged at 15,000 × *g* for 10 min and the clear supernatant was analyzed by high performance liquid chromatography (HPLC). The HPLC system consisted of a Waters X Select CSH C18 3.5 µm 4.6 × 150 mm column with 0.1% trifluoroacetic acid in acetonitrile (60:40, v/v) as a mobile phase, using a flow rate of 1 mL/min. The injection volume was 20 µL and mTHPC was detected by a UV-VIS detector set at 423 nm at a retention time of about 3 min. The measuring range was from 0.05 µg/mL to 25 µg/mL and the detection limit was about 10 ng/mL. A calibration curve was obtained from a series of standard solutions of mTHPC in Foscan diluent to which 60 µL of Balb/c mice plasma was added. Acetonitrile: DMSO (4:1 v/v) was used to extract mTHPC and the collected supernatant was analyzed by HPLC as described above.

Data are presented as the percentage injected mTHPC dose in blood (%ID) over time. On average, Balb/c nude mice have around 58.5 mL of blood per kg of bodyweight. Therefore, the total blood volume (1–1.5 mL) of each individual mouse was calculated by multiplying its bodyweight by 58.5 mL/kg.

2.10.2. Biodistribution in atherosclerotic mice

$LDLR^{-/-}$ $ApoB^{100/100}$ mice were kept on high cholesterol diet (42% of calories from fat and 0.15% from cholesterol, no sodium cholate; TD 88173 Harlan Teklad, Boxmeer, NL) for 5 months to develop atherosclerotic lesions. Food and water were provided ad libitum during the entire study. All animal experiments were approved by National Experimental Animal Board of Finland and carried out in accordance with guidelines of the Finnish Act on Animal Experimentation. For the micelle injections, mice were anaesthetized with isoflurane (induction: 4.5% isoflurane, 450 mL air, maintenance: 2.0% isoflurane, 200 mL air; Baxter International, Helsinki, Finland). Hundred µL of each solution was injected into the tail vein. After 4 h, mice were sacrificed using carbon dioxide anesthesia, perfused with PBS and 1% PFA solution, and aortas and other organs were collected for microscopy analysis. The fluorescence was analyzed from longitudinal sections from aortas or cryo-sections from other tissues with LSM 700 confocal microscope (Carl Zeiss, Jena, Germany).

3. Results

3.1. Micelle preparation

The synthesis and characterization of poly(ε-caprolactone)-*b*-methoxypoly(ethylene glycol) block copolymers is described in Supplementary material. Micelles were conveniently prepared by hydration of a solid polymer film in phosphate buffered saline pH 7.4. The size and size distribution of empty micelles made from Ben-PCL_7-$mPEG_{45}$, Ben-PCL_{11}-$mPEG_{45}$, Ben-PCL_{14}-$mPEG_{45}$ and Ben-PCL_{19}-$mPEG_{45}$ are summarized in Table S2 (Suppl. mater.). Ben-PCL_7-$mPEG_{45}$ micelles prepared at 10 mg/mL polymer concentration had a size of 16 nm and a narrow size distribution (low PDI), while the size increased to 57 nm for the largest Ben-PCL_{19}-$mPEG_{45}$ copolymers. At the same time, an increase is seen in the polydispersity of the micelles, suggesting the formation of larger aggregates with increasing CL block length. DSC

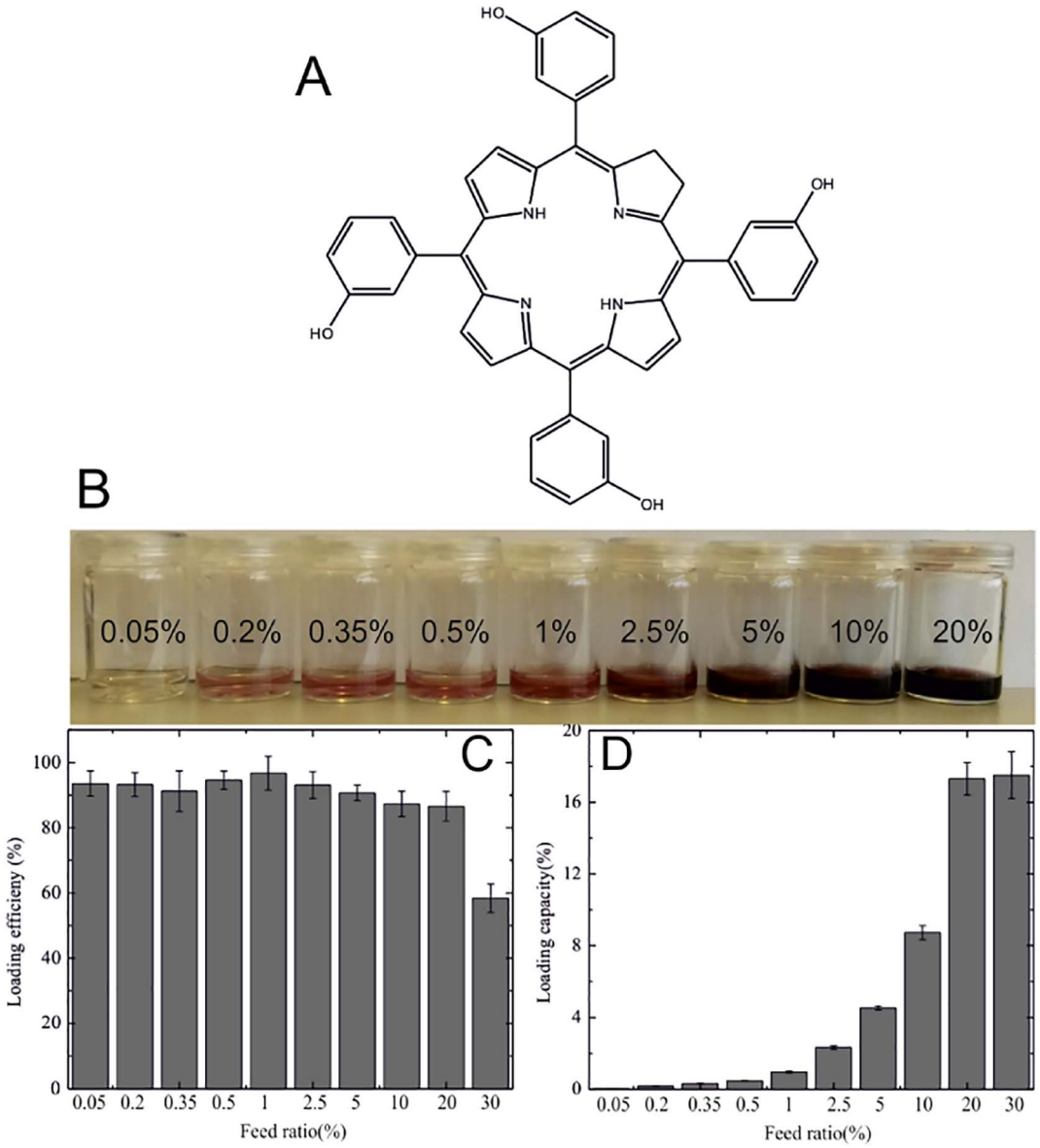

Fig. 1. A) Structural formula of mTHPC. B) 10 mg/mL micellar dispersions of Ben-PCL_7-$mPEG_{45}$ in PBS, loaded with different feed ratios of mTHPC (wt%). C) Loading efficiency of Ben-PCL_7-$mPEG_{45}$ (10 mg/mL dispersions) for mTHPC at different feed ratios (wt%) in in PBS. D) Loading capacity of 10 mg/mL Ben-PCL_7-$mPEG_{45}$ micelles for mTHPC at different feed ratios in PBS dispersions. N = 3.

data of Table S2 shows that the T_m of the PCL block in Ben-PCL_7-$mPEG_{45}$ copolymer is 13.0 °C and increases to 42.7 °C in Ben-PCL_{14}-$mPEG_{45}$ (for Ben-PCL_{19}-$mPEG_{45}$ the PCL T_m overlapped with the PEG T_m at 45.7 °C). Also the ΔH_m of the PCL block increases from 5.1 J/g in Ben-PCL_7-$mPEG_{45}$ to 14.7 J/g in Ben-PCL_{14}-$mPEG_{45}$. Both the increase in T_m and ΔH_m of the PCL block demonstrates that the degree of crystallinity increases with increasing PCL block length.

Due to the small and uniform size and low T_m, Ben-PCL_7-$mPEG_{45}$ was selected for the preparation of mTHPC loaded micelles and for in vitro experiments. The critical micelle concentration of Ben-PCL_7-$mPEG_{45}$, determined by the pendant drop method was 0.04 mg/mL (Fig. S2), which is comparable to other Ben-PCL-PEG block copolymers with a similar PCL/PEG ratio (Carstens et al., 2007).

3.2. Preparation and characterization of mTHPC loaded micelles

Micelles of Ben-PCL_7-$mPEG_{45}$ loaded with mTHPC (Fig. 1A) were prepared using the same film hydration method as for the empty micelles (Carstens et al., 2007). Fig. 1B shows micellar dispersions obtained with different feed ratios from 0.05 to 20% of mTHPC. Loading efficiencies of these dispersions were approximately 90% for these feed ratios (Fig. 1C) and a loading capacity of 17% could be obtained at a feed ratio of 20% (Fig. 1D). Fig. 1D shows that a higher feed ratio of 30% did not result in further increased loading, corresponding with a drop in the loading efficiency (Fig. 1C). This indicates that Ben-PCL_7-$mPEG_{45}$ micelles have a maximum loading capacity of 17% for mTHPC based on polymer-PS weight ratio. Most importantly, Fig. S3 shows that the absorbance spectrum of the loaded micelles at 20% feed ratio resembles the spectrum of an mTHPC solution in DMF, from which it can be concluded that no aggregation occurred of the mTHPC that is encapsulated in the micelles, even at such high loadings.

For demonstration of the photosensitizing ability of the mTHPC-loaded micelles, $^1O_2$ generation was studied upon illumination of the micellar dispersion with broadband light of > 455 nm. As one of the main reactive species in PDT, the rate of $^1O_2$ production is a critical parameter when characterizing new photosensitizers. $^1O_2$ quantum yields (Φ_Δ) were determined in D_2O using the relative method as described by Nombona et al. (Nombona et al., 2012). Fig. S4 (see

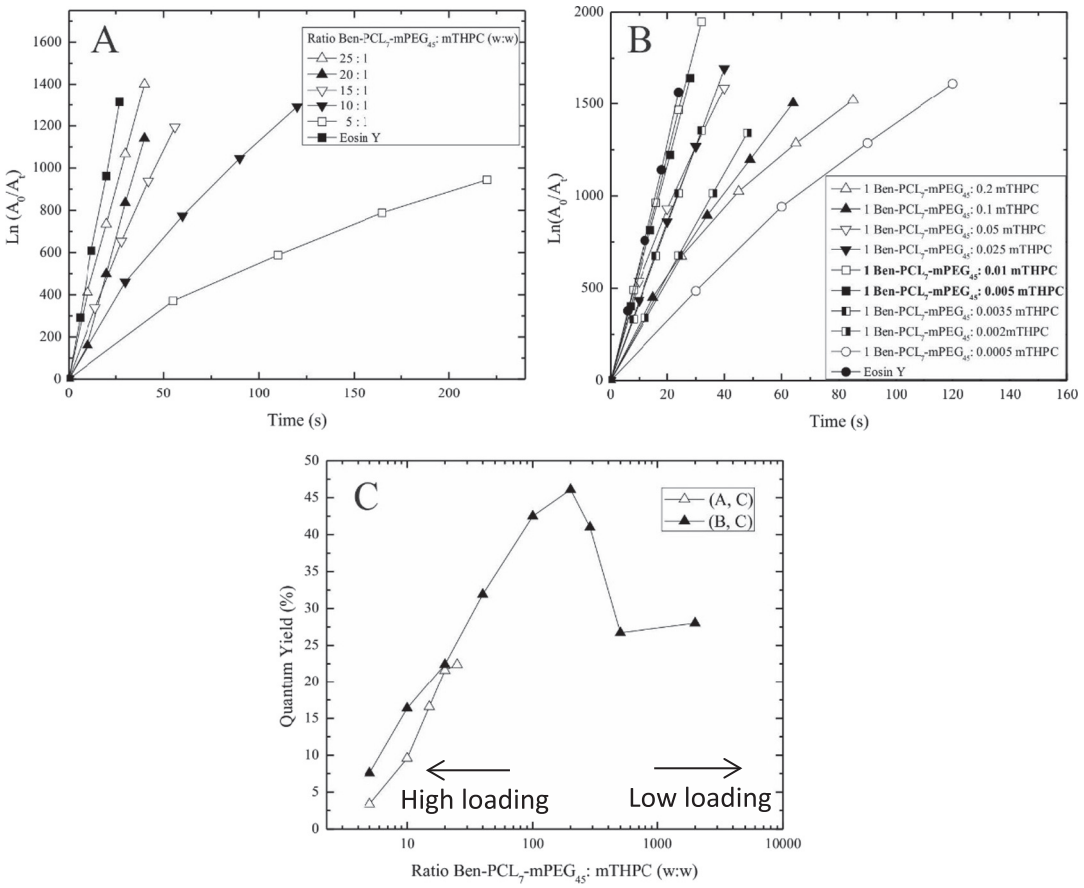

Fig. 2. (A, B) Plot of the decrease in ADMA absorption induced by mTHPC-loaded micelles with varying ratios and (C) corresponding singlet oxygen quantum yield (QY) values obtained from the slope of lines represented in (A,B), of: (A,C) Ben-PCL_7-$mPEG_{45}$:mTHPC (w:w) ratios where the amount of Ben-PCL_7-$mPEG_{45}$ was changed (2–10 mg/mL) and the amount of mTHPC remained constant (0.4 mg/mL); (B,C) Ben-PCL_7-$mPEG_{45}$:mTHPC (w:w) ratios where the amount of mTHPC was changed (0.005–2 mg/mL) and the concentration of Ben-PCL_7-$mPEG_{45}$ was kept constant (10 mg/mL).

Supplementary material) shows an example of the decay of the scavenger absorption during these experiments. Neither decrease in Q-band intensity nor appearance of new bands were observed, confirming the photochemical integrity of the sensitizer during illumination and subsequent formation of $^1O_2$. Plotting the dependence of $\ln(A_0/A_t)$ against irradiation time (t) affords a straight line whose slope reflects the photosensitizer efficacy to generate $^1O_2$, and from which Φ_Δ can be calculated. Fig. 2A–B represents the scavenger photo-degradation profiles induced by two series of samples obtained from stock solutions with varying ratios of Ben-PCL_7-$mPEG_{45}$ or mTHPC, respectively, and the other component's concentration remaining constant. The corresponding Φ_Δ(%) values are summarized in Fig. 2C. Before measurement, all micelle samples were diluted with PBS in D_2O to a similar mTHPC concentration with an absorption of around 0.1 at the Q-band.

First, stock solutions with a fixed amount of mTHPC (0.4 mg/mL) and varying Ben-PCL_7-$mPEG_{45}$ concentrations (2–10 mg/mL, i.e. relatively high feed ratio of 4–20%) were used. These samples were approx. Diluted in 100 times D_2O. Fig. 2C (open triangles) shows that with increasing polymer to mTHPC ratio, i.e. with decreasing photosensitizer loading per micelle, an increasing quantum yield was obtained. When the polymer amount was fixed at 10 mg/mL and the amount of encapsulated mTHPC was decreased over a broader feed ratio (0.05–20%), the Φ_Δ value showed an optimum at a ratio of 200:1 Ben-PCL_7-$mPEG_{45}$:mTHPC (w:w) or 0.5% loading (Φ_Δ = 0.46, see Fig. 2C, closed triangles, and Table S3 in the Supplemental information).

3.3. In vitro cellular uptake and photo-cytotoxicity of mTHPC loaded micelles

A micellar photosensitizer formulation composed of 0.5 mg/mL Ben-PCL_7-$mPEG_{45}$ and 0.1 mg/mL mTHPC (20% loading) showed no dark toxicity on murine RAW264.7 macrophage cells and C166 endothelial cells after an incubation time of 24 h (MTS assay, see Fig. S5). For photocytotoxicity measurements, the cells were not washed for removal of non-internalized micelles but directly illuminated for 10 min after predetermined incubation times (1, 2, 4, 8 or 24 h) with micellar photosensitizer formulations composed of 0.5 mg/mL Ben-PCL_7-$mPEG_{45}$ polymer and 2.5 μg/mL mTHPC (0.5% loading). Fig. 3 shows an increase in photo-cytotoxicity in time for the RAW264.7 macrophages. After 24 h incubation with the photosensitizer formulation, the macrophages were almost completely killed by the generated $^1O_2$, while the C166 endothelial cells hardly showed cell death under the same conditions.

To investigate the rate of uptake of mTHPC in its micellar form by RAW264.7 macrophages and C166 endothelial cells, fluorescence microscopy was performed at several time points (Fig. 4). Because the low photosensitizer concentration used for photocytotoxicity (2.5 μg/mL of mTHPC) gave minimal fluorescence, a higher concentration of 25 μg/mL mTHPC was taken. The pictures clearly show that the fluorescent photosensitizer is associated with both the macrophage and endothelial cells. The darker cores in the cells represent the cell nuclei which are

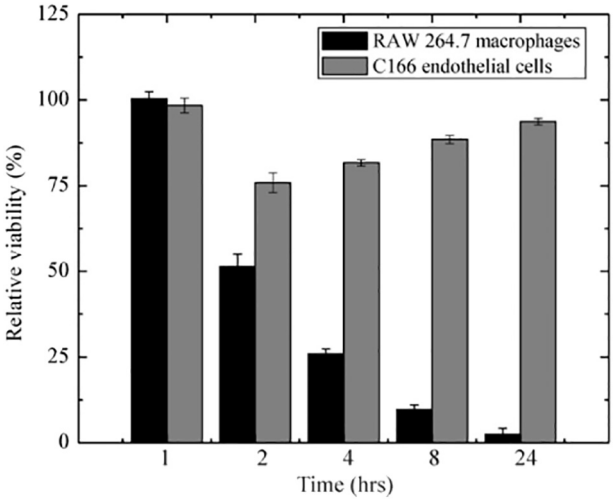

Fig. 3. Photo-cytotoxicity by MTS assay of RAW264.7 macrophages and C166 endothelial cells incubated with micelles composed of 0.5 mg/mL Ben-PCL_7-$mPEG_{45}$ and 2.5 μg/mL mTHPC. After 1, 2, 4, 8 and 24 h of incubation, the cells were illuminated for 10 min, 3.04 mW/cm^2 (n = 3).

not stained by the mTHPC because it cannot penetrate to the nucleus. From this it can be concluded that the photosensitizer is in the cytosol and not associated with the cell surface.

To obtain more information about the mechanism of photoinduced cell killing, and which formulation factors play a major role in that, both polymer concentration and mTHPC concentration were systematically varied and photo-cytotoxicity was studied using RAW264.7 macrophages and C166 endothelial cells. According to Fig. S6 and S7 (Supplementary material), when the polymer concentrations were fixed below the CMC (i.e. 0.04 mg/mL) the IC50 is hardly dependent on the polymer concentration. As expected, this indicates that the micelles dissociated and the PDT effect is caused by the released photosensitizer. Those IC50 values were a bit higher for C166 endothelial cells (approximately 0.3 μg/mL mTHPC) as compared to RAW264.7 macrophages, which had an IC50 of 0.08 μg/mL. This indicates that C166 endothelial cells are less sensitive to singlet oxygen generation or have a lower uptake rate of the free mTHPC. Surprisingly however, above the CMC, i.e. in the presence of intact micelles, not only the mTHPC but also the polymer concentration plays an important factor in the cell killing potential, i.e. the IC50 values increased with increasing polymer concentration. For example, in Fig. 5 it can be seen that 0.1 mg/mL polymer and 0.35 μg/mL mTHPC gave major cell killing after illumination (cell viability of only 26%), while the same mTHPC concentration but with a higher polymer concentration of 0.5 mg/mL did not kill the RAW264.7 cells at all under these conditions (i.e. 125% cell viability). Most importantly, the IC50 values were also cell type dependent. A similar polymer concentration dependency was observed for the C166 endothelial cells, but above the CMC (0.04 mg/mL) the amount of mTHPC that is needed to give similar photo-cytotoxicity (i.e. IC50 value) is approximately one order of magnitude higher (Fig. 5).

Photocytotoxicity for RAW264.7 macrophages was also investigated with micelles composed of Ben-PCL_n-$mPEG_{45}$ with increasing PCL blocks lengths (n) of 7, 11, 14 or 19 units. The concentration of the micelles was kept at 0.5 mg/mL, the concentration of mTHPC was 1.75 μg/mL and incubation time was 24 h. In Fig. 6 it is clearly seen that upon increasing the PCL block length, the relative viability of the macrophages also increased and thereby increasing the IC50 value of mTHPC.

Previous results have shown that mTHPC-loaded PCL-based micelles can be degraded by lipases, thus releasing the photosensitizer and induce cell killing upon illumination (Hofman et al., 2008). In Fig. 7, the lipase activity of both RAW264.7 macrophages and C166 was investigated using a colorimetric assay. It is seen that the RAW macrophages have a lipase activity of 12 milliunits/mL while the C166 cells display a lipase activity of 6.6 milliunits/mL.

3.4. In vitro stability of mTHPC–loaded micelles in serum and plasma

Fluorescence properties of micellar and liposomal formulations of mTHPC were evaluated in PBS and compared with Foscan® (free mTHPC in solvent). Fig. 8A shows the intensity of fluorescence of mTHPC in these samples as a function of mTHPC concentration. For the micelles, the range of concentrations was obtained by varying the loading % of mTHPC at a fixed polymer concentration (10 mg/mL), while for the liposomes a dilution series in PBS was obtained from a stock solution of Foslip®, thus keeping the loading % (i.e. mTHPC/lipid ratio) constant upon dilution. The fluorescence of mTHPC loaded micelles increased almost linearly with increasing mTHPC concentration ranging from 0.001 to 0.005 mg/mL (loading from 0.1 to 0.5% w/w), with similar intensity as for free mTHPC in Foscan® at the same concentrations. At higher loading %, the fluorescence of mTHPC loaded micelles showed a rapid decrease with increasing mTHPC loading, while the fluorescence intensity of Foscan® showed a gradual upward trend until it levelled off at 0.1 mg/mL. The fluorescence from Foslip® is lower than that of Foscan® in the whole mTHPC concentration range. The fluorescence of Foslip® did hardly change when diluted in PBS from 0.2 to 0.025 mg/mL of mTHPC (Fig. 8A). However, only with further dilution of Foslip® in PBS, mTHPC fluorescence started to decrease. The fluorescence of mTHPC loaded micelles at different loadings and Foslip® dilutions in PBS was stable in time over 8 h at 37 °C (see Supplementary Fig. S8). When Foscan diluent (ethanol:propylene glycol, 40/60 w/w%) was added to the micelles or to Foslip® at mTHPC concentration of 0.2 mg/mL to destroy the particles, the fluorescence was restored to almost the same level as Foscan® (data not shown).

The stability of the three formulations (Foscan®, Foslip® and micelles) at 0.2 mg/mL mTHPC was assessed in diluted serum (FBS), mouse plasma and human plasma by the change in fluorescence over time at 37 °C(Fig. 8B–D). Upon addition to plasma or serum, the fluorescence of Foscan® was lower than in organic solvent (ethanol:propylene glycol, 40/60 w/w%) (compare Fig. 8A with Fig. 8B–D) but remained quite constant in time in different amounts of mouse and human plasma (Fig. 8, red lines). Only a slight increase of the Foscan® fluorescence was observed in the first 1 h incubation in FBS solutions and then remained stable. The fluorescence of Foslip® (black lines in Fig. 8B–D) increased gradually in FBS, human plasma and mice plasma in the first 2 or 3 h of incubation, which was more pronounced with higher serum or plasma concentrations, and then remained stable. For the micellar formulation with 20% loading (blue lines in Fig. 8B–D), a rapid increase of fluorescence was observed within the first 30 min of incubation and then levelled off, which was more significant with increasing serum or plasma concentration from 10% to 90%, reflecting a burst release of mTHPC from the micelles.

The changes of fluorescence in time at lower mTHPC concentrations (0.025, 0.05 and 0.1 mg/mL) for the micelles, liposomes and free mTHPC in 10, 50 and 90% of FBS, human plasma and mouse plasma are shown in Supplementary Fig. S9. The trends are similar as for the higher mTHPC concentration shown in Fig. 8: the constant fluorescence of Foscan® (Fig. S9 red lines), the progressive increase of fluorescence from Foslip® in the first 2 or 3 h of incubation (black lines in Fig. S9), and a rapid increase of fluorescence for the micellar formulations at the first 30 min incubation (blue lines in Fig. S9), were all independent of the mTHPC concentration.

The final fluorescence intensities of the three formulations with a series of mTHPC concentrations after 8 h incubation in the different media are summarized in Table 1. The fluorescence of free mTHPC (Foscan®, Table 1A) increased with increasing FBS concentration, and was more significant in mouse plasma and even slightly more in human plasma, except for the lowest mTHPC concentrations. Fluorescence generally increased when Foscan® was more diluted at a fixed serum or

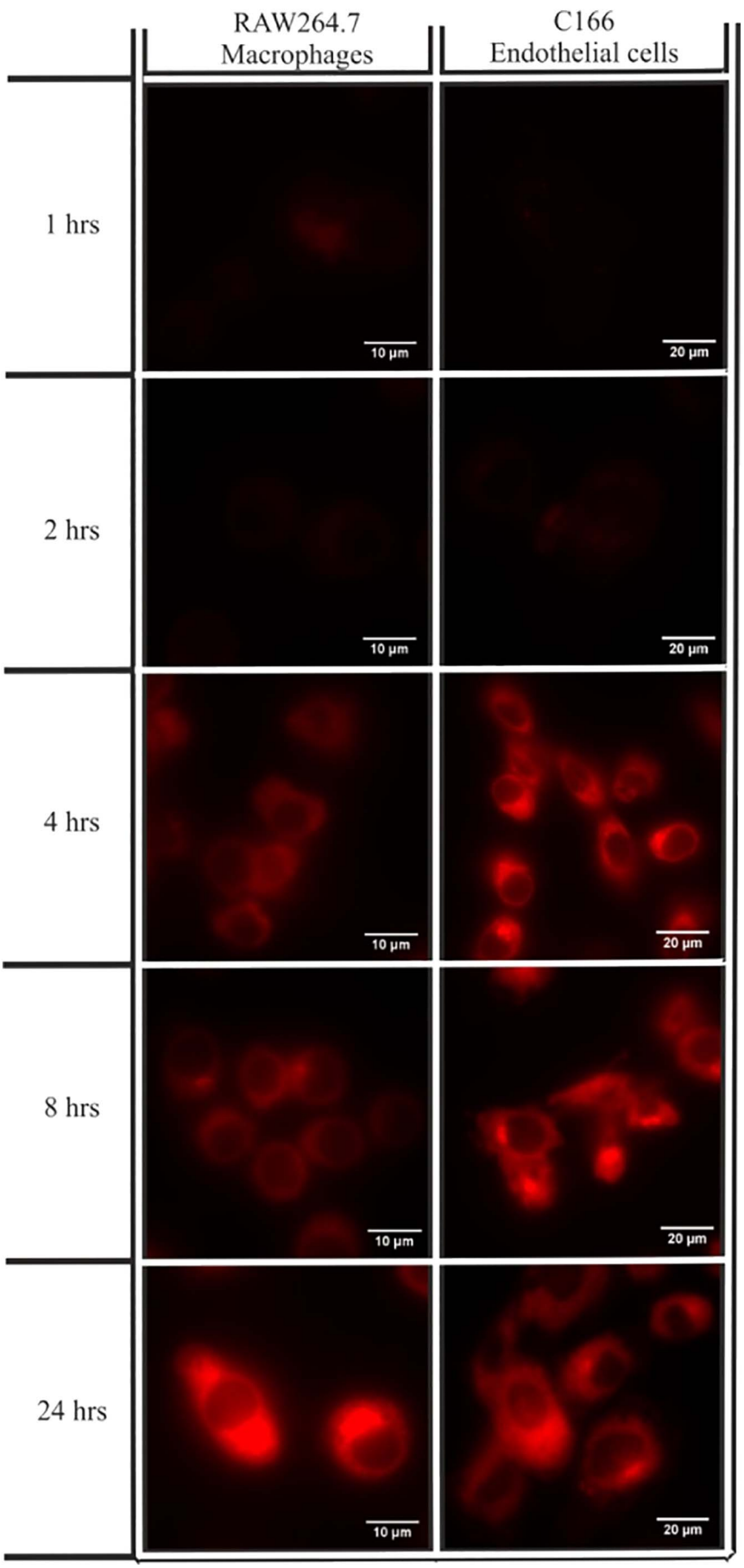

Fig. 4. Fluorescence image of RAW264.7 macrophages and C166 endothelial cells incubated with micelles composed of 0.5 mg/mL Ben-PCL_7-$mPEG_{45}$ polymer and 25 µg/mL mTHPC after 1, 2, 4, 8 and 24 h. The cells were not illuminated to preserve cell morphology for the microscope pictures.

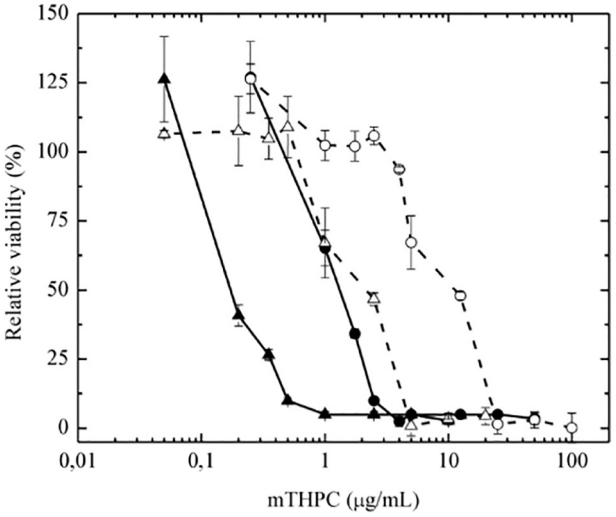

Fig. 5. Photocytotoxicity by MTS assay at fixed polymer concentrations above the CMC and varying mTHPC loadings on RAW264.7 macrophages and C166 endothelial cells after 24 h of incubation. The cells were illuminated for 10 min, 3.04 mW/cm^2. —●— RAW264.7 Macrophages, 0.5 mg/mL Ben-PCL$_7$-mPEG$_{45}$, - ○ - C166 endothelial cells, 0.5 mg/mL Ben-PCL$_7$-mPEG$_{45}$, —▲— RAW264.7 Macrophages, 0.1 mg/mL Ben-PCL$_7$-mPEG$_{45}$, - △ - C166 endothelial cells, 0.1 mg/mL Ben-PCL$_7$-mPEG$_{45}$. N = 3.

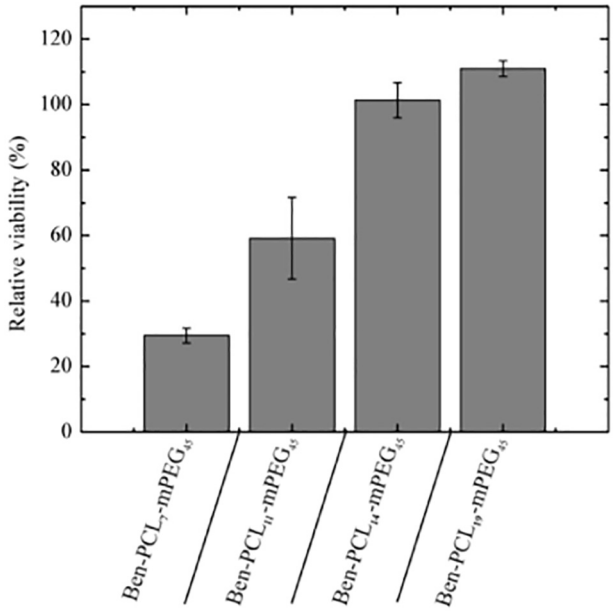

Fig. 6. Photo-cytotoxicity by MTS assay of 0.5 mg/mL polymer with varying PCL block lengths, and 1.75 μg/mL mTHPC, on RAW264.7 macrophages after 24 h of incubation. The cells were illuminated for 10 min, 3.04 mW/cm^2. N = 3.

plasma concentration. When the lowest concentration (0.025 mg/mL) was added to the highest amount of mouse or human plasma (90%), fluorescence intensity levelled off to a maximum value of 3400 a.u., similar to that of free mTHPC in organic solvent (3500 a.u.: see red line in Fig. 8A at this concentration), which was also the case with 0.05 mg/mL in 90% human plasma (3800 a.u. versus 4100 a.u. in organic solvent).

For Foslip® with different mTHPC concentrations (Table 1B), the increase of fluorescence with increasing serum or plasmas concentrations was observed as well, again following the order in human plasma > mouse plasma > FBS. Also here, the values levelled off at 50 to 90% serum or plasmas at the lower mTHPC concentrations. Overall, the intensities of Foslip® at given mTHPC concentrations were higher than that of Foscan®.

As shown in Table 1C, decreasing the loading % of mTHPC loaded

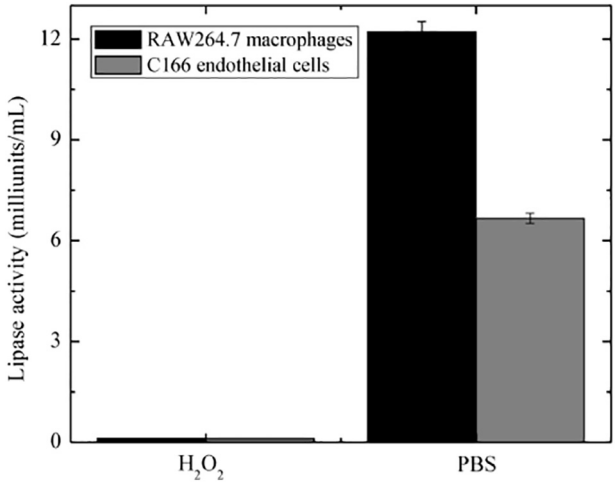

Fig. 7. Lipase activity in RAW264.7 macrophages and C166 endothelial cells measured in PBS. H_2O_2 treated cells were used as a negative control. N = 3.

micelles led to increase of the fluorescence intensity from 0 to 1.600 a.u. in 0% plasma or serum (pure PBS, same data as in Fig. 8A). Remarkably, addition of micelles to plasma or serum resulted in similar FI as for free mTHPC (compare Table 1C with 1A). As for free mTHPC, the fluorescence from mTHPC loaded micelles increased with increasing FBS concentration and was more significant in mouse and human plasma. For all loading%, fluorescence intensity increased around 300 units from 10 to 50% FBS and another 400 units from 50 to 90% FBS. In mouse plasma, FI of micelles with 0.2 mg/mL (20% loading) and 0.1 mg/mL mTHPC (10% loading) increased 4–7 times from 10 to 50% plasma and then increased another 1.5 times when increasing to 90% plasma. The lower loadings seemed to level off at around 3200 a.u. when mouse plasma concentrations were increased. Similar trends were observed in human plasma but with slightly higher absolute fluorescence intensities compared to that in mouse plasma.

3.5. *In vivo* pharmacokinetics and biodistribution of mTHPC loaded micelles in mice

The pharmacokinetic profiles of mTHPC loaded micelles were determined from blood samples after intravenously administering micelles with 5.0 and 0.6% mTHPC loading (w/w) to Balb/c nude mice via tail vein (Fig. 9). The "low dose" formulation with 0.6% mTHPC loading was chosen to give a systemic concentration upon *i.v.* injection in mice of approx. 0.6 mg/mL Ben-PCL$_7$-mPEG$_{45}$ and 4 μg/mL mTHPC, which were the similar concentrations that gave the highest macrophage selectivity in vitro. The "high dose" formulation with 5% mTHPC loading would give the same systemic concentration of polymer (around 0.6 mg/mL Ben-PCL$_7$-mPEG$_{45}$) but 8 times higher concentration of mTHPC (approx. 32 μg/mL). mTHPC loaded micelles in low dose group exhibited slightly higher mTHPC levels in the circulation for the first 5 min as compared to the high dose group, but decay profiles were similar for both mTHPC formulations. According to the semi-logarithmic plot (insert Fig. 9), these profiles followed first order kinetics, the slope corresponding with half-life times ($t_{1/2}$ values) of 1.5 h. The corresponding mTHPC plasma concentrations at low and high dose were 4.9 and 32.4 μg/mL, respectively, at 5 min, which decreased to 0.74 and 4.74 μg/mL at 4 h.

Similar two samples (high and low dose) as used in pharmacokinetic study were selected for determination of the biodistribution in atherosclerotic LDLR$^{-/-}$ ApoB$^{100/100}$ mice in vivo. Directly after *i.v.* injection, the "low dose" formulation gives a systemic concentration in mice of 0.5 mg/mL Ben-PCL$_7$-mPEG$_{45}$ and 4 μg/mL mTHPC, while the "high dose" formulation would give the same systemic concentration of polymer (0.5 mg/mL Ben-PCL$_7$-mPEG$_{45}$) and 25 μg/mL mTHPC. The

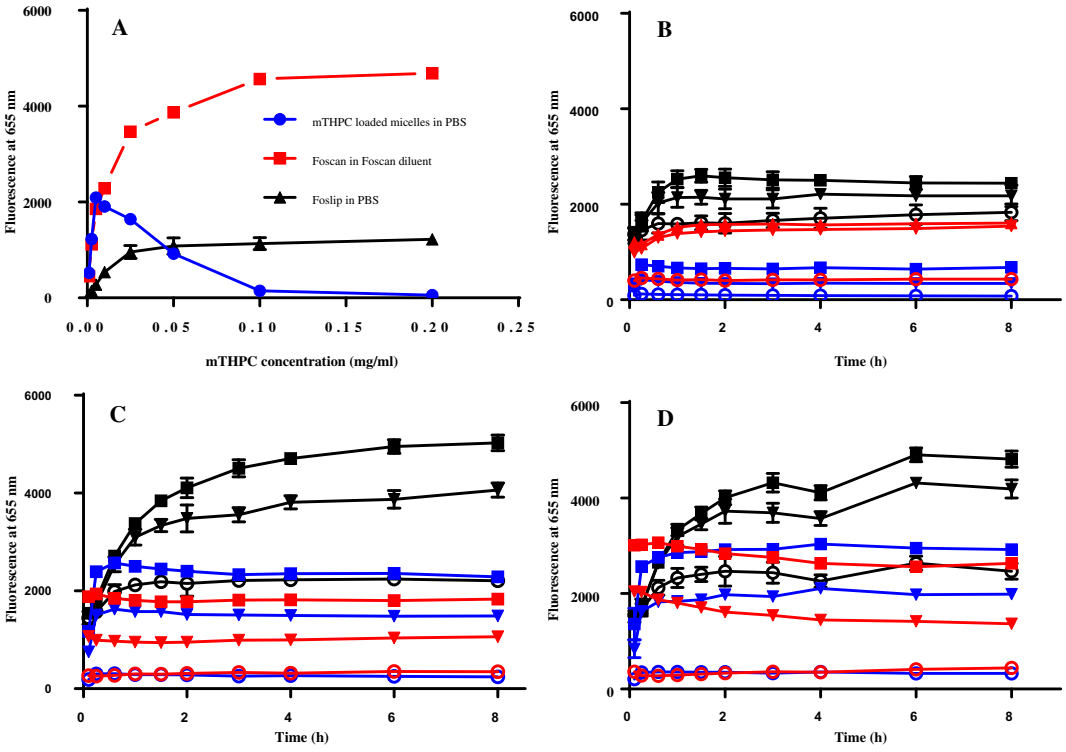

Fig. 8. A) Fluorescence intensity (λ_{ex} 420 nm, λ_{em} 655 nm) as a function of mTHPC concentration; Foscan® and Foslip® stock solutions were diluted in ethanol: propylene glycol (40:60 w/w%) and PBS (pH 7.4), respectively, while micelles of 10 mg/mL with different loading amounts (0.1–20% w/w) were individually prepared and each diluted 10 × in PBS to obtain the corresponding mTHPC concentrations. B)–D) Fluorescence intensity as a function of time at mTHPC concentration of 0.2 mg/mL in FBS (B), mouse plasma (C), human plasma (D); Foscan®, Foslip® and mTHPC loaded micelles were 10 × diluted with FBS or plasma solutions and incubated while the mTHPC fluorescence was recorded at 37 °C over a period of 8 h (in duplicate). In B)–D) black lines, red lines and blue lines represent Foslip®, Foscan® and mTHPC loaded micelles, respectively. Squares, triangles and open dots are for all samples in 90, 50 and 10% FBS or plasma, respectively. (For interpretation of the references to color in this figure legend, the reader is referred to the web version of this article.)

Table 1
Fluorescence intensities (FI, a.u. × 10^3) (λ_{ex} 420 nm, λ_{em} 655 nm) of Foscan® (A), Foslip® (B) and mTHPC loaded micelles (C) with various mTHPC concentrations after 8 h incubation in diluted (0, 10, 50 and 90% in PBS) fetal bovine serum (FBS), mouse plasma (MP) and human plasma (HP).

A	Foscan® FI in FBS				Foscan® FI in MP			Foscan® FI in HP		
[mTHPC] (mg/mL)	0%*	10%	50%	90%	10%	50%	90%	10%	50%	90%
0.025	0	1.1	1.6	2.2	1.0	3.3	3.4	1.7	3.3	3.4
0.050	0	1.3	1.5	1.8	0.8	2.6	3.2	1.1	3.2	3.8
0.100	0	0.8	1.6	1.6	0.6	1.7	3.0	0.7	2.8	3.6
0.200	0	0.4	1.5	1.6	0.4	1.1	1.8	0.4	1.4	2.6

B	Foslip® FI in FBS				Foslip® FI in MP			Foslip® FI in HP		
[mTHPC] (mg/mL)	0%*	10%	50%	90%	10%	50%	90%	10%	50%	90%
0.025	1.0	1.8	2.8	2.7	2.5	3.3	3.3	3.5	4.2	4.1
0.050	1.1	1.7	2.6	2.8	2.4	3.7	3.9	3.7	4.9	4.9
0.100	1.1	1.9	2.6	3.0	2.2	4.8	5.2	2.8	4.6	4.9
0.200	1.2	1.8	2.2	2.4	2.2	4.0	5.0	2.5	4.2	4.8

C	Micelles FI in FBS				Micelles FI in MP			Micelles FI in HP		
[mTHPC] (mg/mL)	0%*	10%	50%	90%	10%	50%	90%	10%	50%	90%
0.025	1.6	1.4	1.7	1.9	1.3	3.2	3.3	1.7	3.3	3.4
0.050	0.9	0.6	0.8	1.3	0.6	2.6	3.2	0.6	3.2	3.7
0.100	0.1	0.1	0.5	1.0	0.3	1.7	2.6	0.5	2.6	3.5
0.200	0.0	0.0	0.3	0.7	0.2	1.5	2.3	0.3	2.0	2.9

* As controls, the fluorescence intensities of Foscan® and Foslip® and mTHPC loaded micelles without serum or plasmas (0%) were obtained by adding 1:9 (v/v) of samples to PBS (pH 7.4).

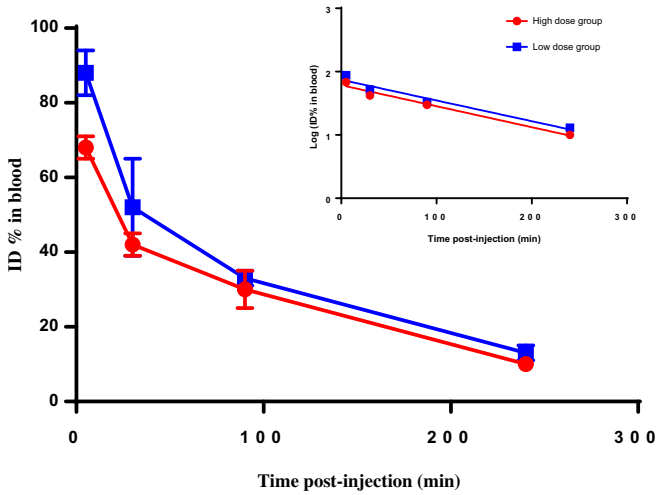

Fig. 9. In vivo pharmacokinetics of mTHPC loaded in micelles based on Ben-PCL_7-$mPEG_{45}$ upon tail vein administration in healthy nude Balb/c mice (mTHPC dosage in high (5% loading) and low (0.6% loading) dose group is 50 μg and 6 μg mTHPC, respectively). Blood samples taken at different time points were used to quantify the percentage of mTHPC injected dose (%ID) present in systemic circulation. The total blood volume of the mice is assumed to be around 1–1.5 mL, depending on bodyweight. The inset shows the log-concentration versus time. Data are presented as mean ± SD, N = 3.

mice were kept on a high fat diet to develop an atherosclerotic lesions for 5 months. 4 h after tail vein injection, the mice were sacrificed, and organs were analyzed with confocal microscopy. mTHPC was present in liver, spleen, kidney and lung in varying degrees (Supplementary Fig. S11). The most interesting result obtained is depicted in Fig. 10. The high dose formulation clearly preferentially located in the atherosclerotic plaque. In the low dose the mTHPC is probably present but the amount of mTHPC is too low to observe any fluorescence, similar as with the fluorescence microscope described earlier.

4. Discussion

We have shown previously that PCL based micelles can be used to encapsulate very high amounts of the photosensitizer mTHPC (Hofman et al., 2008). Encapsulation reduced the uptake and photocytotoxicity with 14C head and neck cancer cells as compared to free mTHPC, which was recovered by dilution of the micelles below the CMC or after enzymatic degradation of the micelles by lipase. Since macrophages generally show elevated lipase activity (O'Brien et al., 1992), these findings triggered us to investigate these formulations for its applicability in the PDT of atherosclerosis, an inflammatory disease. As opposed to our previous work, for simplicity, we did not fractionate the polymers to obtain monodisperse polymers, but just took the polydisperse ones as prepared. Also the length of the PEG block was increased from 750 to 2000 Da and the synthesis route was modified. Despite that, the size of the empty micelles with average number of 7 caprolactone units (16 nm) was very similar to the micelles of the monodisperse polymers with the same (exact) number of CL units (Carstens et al., 2007). Also the melting temperature of the polymer (13 °C) was in accordance with the previously obtained results; block copolymers of Ben-PCL_4-PEG_{17} with monodisperse PCL blocks had a PCL melting temperature at − 25 °C which increased upon an increase of the PCL block to 10 °C for 6 CL units. The observed increase in PDI when the PCL chain length increased beyond 7 correlated with the increased T_m and ΔH_m (table S2), and can therefore be attributed to the higher tendency to form crystals and thus larger aggregates for the larger block copolymers.

The maximum loading capacity of the micelles for mTHPC (17 wt%) was again similar to Hofman et al. for the loading capacity of Ben-PCl_5-PEG_{17} with monodisperse PCl blocks at 20% feed ratio of mTHPC (Hofman et al., 2008). As opposed to our new results, loading capacity in those micelles based on Ben-PCl_5-PEG_{17} could be further increased to 30 wt%, at 30% feed ratio of mTHPC. A possible explanation for this difference is the ratio of PCL/PEG. The Ben-PCl_5-PEG_{17} of Hofman et al. has 43 wt% PCL and the current Ben-PCL_7-$mPEG_{45}$ copolymer has only on average 28 wt% PCL. Due to lower hydrophobicity in the Ben-PCL_7-$mPEG_{45}$ system, the extreme high loading capacities such as in Ben-PCl_5-PEG_{17} were not obtained. In any case, the absence of aggregation of mTHPC inside the micelles (see Fig. S3) is very important and promising, since aggregation of photosensitizers often hampers singlet oxygen generation (Tanielian et al., 2001). Despite the fact that even at the highest loading (20% w/w) we observed no aggregation by UV–vis spectroscopy, quenching of the fluorescence of the mTHPC in the micelles was observed above 0.5% w/w loading (Fig. 8A: 0.005 mg/mL mTHPC in 1 mg/mL polymer dispersion). The fluorescence intensity nicely correlates to the singlet oxygen quantum yield: both show their highest values at a loading of 0.5% w/w (200:1 polymer to mTHPC ratio) (compare Fig. 8A and 2C). In those best conditions, the singlet oxygen quantum yield values obtained approached those of the best PDT photosensitizers in the literature (Zhu et al., 2014), encouraging us to further study the use of mTHPC-loaded micelles for PDT treatment of atherosclerosis.

Photocytotoxicity experiments revealed a much larger sensitivity of the macrophages as compared to the endothelial cells. After the incubation with the mTHPC loaded micelles, the cells were not washed

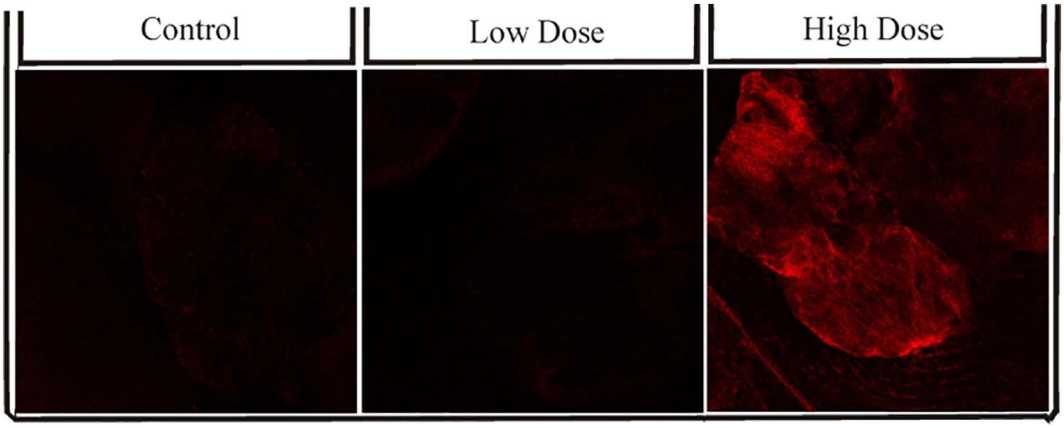

Fig. 10. Confocal fluorescence images of atherosclerotic lesions in $LDLR^{-/-}$ $ApoB^{100/100}$ mice aorta's, taken 4 h post injection of formulations in the tail vein. The control group was injected with PBS. In the low mTHPC dose, 100 μL of a solution containing 1 mg Ben-PCL_7-$mPEG_{45}$ and 8 μg mTHPC in PBS was injected, resulting in a systemic concentration of 0.5 mg/mL Ben-PCL_7-$mPEG_{45}$ and 4 μg/mL mTHPC. In the high mTHPC dose, 100 μL of solution containing 1 mg Ben-PCL_7-$mPEG_{45}$ and 50 μg mTHPC in PBS was injected, resulting in a systemic concentration of 0.5 mg/mL Ben-PCL_7-$mPEG_{45}$ and 25 μg/mL mTHPC. The total blood volume of the mice is assumed to be 2 mL.

for removal of non-internalized micelles but directly illuminated for 10 min in the presence of the micellar dispersions. In other words, total mTHPC concentration (extracellular plus intracellular) was the same in all experiments. Therefore, if the singlet oxygen generated by the photosensitizer is similarly active outside and inside the cells, the photo-cytotoxicity would be independent of the incubation time. However, Fig. 3 clearly shows an increase in photo-cytotoxicity in time for the RAW264.7 macrophages, most likely related to the increasing extend of internalization. This indicates that the uptake of the photosensitizer plays an important role in the cell killing of RAW264.7 macrophages. Interestingly, in Fig. 3 it is clearly visible that RAW264.7 macrophages are efficiently killed after 24 h incubation by the generated singlet oxygen, while the C166 endothelial cells hardly show cell death under the same conditions. Nevertheless, the fluorescence microscopy pictures, especially after 4 and 8 h, suggest that the uptake rate by C166 endothelial cells is even slightly faster than by RAW264.7 macrophages, which is not in accordance to the photocytotoxicity results. This suggests that after uptake of loaded micelles another process is active inside macrophage cells, and not in C166 cells, that results in the observed selective cell killing after illumination. Because in our previous work we have seen that the mTHPC only became photoactive after degradation of the micelles by lipase (Hofman et al., 2008), we measured the lipase activity of both cell lines and corroborated that macrophages indeed showed higher lipase activity (Fig. 6). This process could therefore very well explain the selective killing of macrophages as compared to the endothelial cells. The lipase-dependent activation of the photosensitizer was further indicated by the observed dependency on the polymer concentration and molecular weight at a fixed mTHPC amount (i.e. the higher the relative polymer amount and the longer the PCL blocks, the longer it takes for the micelles to fully degrade and release the photosensitizer), and by the fact that the polymer concentration and the cell type dependency of the IC50 values were only observed above the polymer's CMC.

This selectivity in cell killing potential is most interesting for the targeting because we want the endothelial layer of atherosclerotic plaques to stay alive. It gives us an opportunity to select a window where it is possible to kill the RAW264.7 macrophages and keep the endothelial layer alive: for example at 0.5 mg/mL polymer concentration and 4 μg/mL mTHPC, 94% of the endothelial cells survived while 95% of the macrophage cells were killed. The same was true for 0.1 mg/mL polymer but then at a lower mTHPC concentration of 0.5 μg/mL (Fig. 5). If the selectivity towards macrophages could be translated to the in vivo situation, it could become a very interesting intervention treatment in the inflammation process of atherosclerosis (Waksman et al., 2008), without harming the endothelial layer.

Before moving to in vivo studies, we first investigated the in vitro stability of the mTHPC micellar formulations in serum and plasma, and compared this with a known commercial liposomal formulation of mTHPC (Foslip®). As shown in Fig. 8A, mTHPC loaded micelles exhibited linear increase in fluorescence intensity with increasing mTHPC loading from 0.1 to 0.5% w/w. However, above 0.5% w/w loading, the sudden decrease in the fluorescence of mTHPC loaded micelles can be attributed to fluorescence quenching resulting from high mTHPC local concentration in micelles. In such case, fluorescence can be restored after destroying the micelles by addition of an surfactant or an organic solvent (Kachatkou et al., 2009). Indeed, this was the case when the micelles or Foslip® were dissolved in Foscan® diluent. As opposed to the loaded micelles, where mTHPC to polymer ratio was varied in Fig. 8A, the liposomes of a Foslip® stock solution were diluted in their entirety keeping a constant mTHPC to lipid ratio. Therefore the fluorescence quenching of mTHPC in Foslip® did not change in PBS (Fig. 8A) because dilution of both mTHPC and lipids does not have an effect of the local concentration inside each liposome. Only when significantly diluted (below 0.025 mg/mL of mTHPC), liposomes may become unstable, thus leading to the decrease of mTHPC fluorescence.

When mTHPC dissolved in an organic solvent (Foscan®) was added to PBS, severe precipitation occurred and fluorescence intensity was completely diminished. However, when added to plasma or serum, part of the mTHPC associated to proteins and remained fluorescent, its intensity depending on the ratio of mTHPC to plasma or serum (Table 1A). When the amount of protein was sufficient to solubilize the amount of mTHPC that was added, the fluorescence intensity coincided with similar concentrations of free mTHPC in organic solvent. The amount of plasma or serum to fully solubilize a certain amount of mTHPC was medium dependent and reflects the order of solubilisation power for mTHPC. The solubilisation power of human plasma > mouse plasma ≫ FBS is probably due to the different amount of proteins in these media.

For the stability studies of micelles and liposomes in serum and plasma, we made use of the quenched state of the fluorescence when mTHPC is present in the micelles (above 0.5% w/w loading) or in the liposomes. Therefore, the observed increase in fluorescence upon incubation in serum or plasma can be attributed to release from the micelles or liposomes and binding to serum or plasma proteins. Foslip® showed a steady increase in fluorescence when incubated for 8 h in serum or plasma regardless of mTHPC concentrations, indicating slow-release. This is consistent with previous studies, where a slow-release of m-THPC from liposomes in 5% human serum was observed (Reshetov et al., 2011). The release of mTHPC from Foslip® is medium and medium concentration dependent (Table 1B). The fluorescence at low mTHPC concentrations (0.025 and 0.01 mg/mL) levelled off at 50 and 90% serum or plasma solutions, indicating release of mTHPC from liposome was complete. The higher intensities of Foslip® compared to Foscan® at corresponding mTHPC concentrations is due to the presence of liposomes which aid in the solubilisation of mTHPC.

All mTHPC loaded micelles, irrespective of the loading%, exhibited a rapid increase in fluorescence intensity in the first 30 min and then remained stable (Fig. 8B-D and Fig. S9). This dequenching process indicates burst release. Like Foslip®, the amount of release of mTHPC from micelles is dependent on medium and medium concentration. At lower mTHPC loading, 2.5% (w/w) for instance, the release is almost complete in 50% FBS or plasmas because fluorescence was similar to that of Foscan® and did not increase significantly more at 90% serum or plasma.

In the pharmacokinetic study, after *i.v.* administration of the mTHPC loaded micelles, the $t_{1/2}$ value is 1.5 h, regardless of mTHPC to polymer ratio (high dose at 5% loading or low dose at 0.6% loading). This is very much consistent with data reported by Cramers et al. after administration of Foscan® (i.e. $t_{1/2}$ is 1.3 h in Balb/c mice) (Cramers et al., 2003), indicating rapid release of mTHPC from the micelles in circulation. This rapid release in vivo is in line with the in vitro release in serum and plasmas, suggesting the importance of pre-testing the in vitro release behavior in plasma for predicting the fate of a delivery system in vivo. This fast release behavior can be caused by high binding affinity of mTHPC with serum and plasma (lipo)proteins leading to mTHPC redistribution from intact micelles to lipoproteins (Polo et al., 2002; Chowdhary et al., 2003; Sasnouski et al., 2005). Also protein binding of polymer unimers can play a role, which in combination with dilution upon injection causes an adverse shift of the micel-unimer equilibrium and the destruction of micelles (Sasnouski et al., 2005; Talelli et al., 2015).

Combined with premature release and concomitant pharmacokinetic profile of mTHPC loaded micelles, the observed fluorescence of the atherosclerotic lesions in mice by accumulated mTHPC (see Fig. 10) is probably due to released mTHPC that subsequently binds to lipoproteins, particularly in low-density lipoprotein (LDL) (Michael-Titus et al., 1995; Reshetov et al., 2012). LDL as an endogenous carrier can be rapidly transported across an intact endothelium and then ingested by macrophages in the form of oxidized LDL particles (Jori and Reddi, 1993; Berliner et al., 1995; Polo et al., 2002). Indeed, it has been reported that the association of photosensitizers with lipoproteins promotes selective accumulation into tumour tissues and atherosclerotic

plaques, thus enhancing their therapeutic potential (Jori and Reddi, 1993; Allison et al., 1997; Konan et al., 2002; Svensson et al., 2007).

5. Conclusions

The photosensitizer mTHPC was loaded in Ben-PCL-mPEG micelles with high efficiency and capacity and without any aggregation of the photosensitizer. mTHPC-loaded micelles' photo-cytotoxicity is induced by the degradation of the PCL block of Ben-PCL-mPEG micelles by lipases. In accordance to their higher lipase activity, RAW264.7 macrophages degrade the micelles faster and thus activate the photosensitizer earlier than C166 endothelial cells, thus creating a window for selective killing of the RAW264.7 macrophages. Despite the selective accumulation of mTHPC in atherosclerotic plaques of mice aorta's, likely due to the proposed binding to lipoproteins, translation from in vitro to in vivo of the beneficial selective macrophage photocytotoxicity was not possible due to the premature release from the micelles. Therefore, our current aim is to improve the stability of mTHPC-loaded PEG-PCL based micelles (e.g. by chemical crosslinking (Van Nostrum, 2011) to fully take advantage of the macrophage selectivity and passive targeting to atherosclerotic plaques. If this aim is achieved, the Ben-PCL-mPEG micelles might be a very interesting delivery system with dual targeting effect, i.e. passive targeting to atherosclerotic lesions and faster degradation by macrophages and thus higher selectivity to PDT compared to healthy endothelial tissue.

Acknowledgements

The research leading to these results has received funding from the European Union Seventh Framework Programme (FP7/2007–2013) under the CosmoPHOS-nano Project, grant agreement no 310337. Financial support from Spanish MINECO (CTQ-2014-52869-P (TT) and CTQ-2014-53673-P (AdlE)) is acknowledged. YL is supported by China Scholarship Council, grant number 201506220178.

Appendix A. Supplementary data

Supplementary data to this article can be found online at http://dx.doi.org/10.1016/j.ejps.2017.06.038.

References

Allison, B.A., Crespo, M.T., Jain, A.K., Richter, A.M., Hsiang, Y.N., Levy, J.G., 1997. Delivery of benzoporphyrin derivative, a photosensitizer, into atherosclerotic plaque of Watanabe heritable hyperlipidemic rabbits and balloon-injured New Zealand rabbits. Photochem. Photobiol. 65, 877–883.

Berliner, J.A., Navab, M., Fogelman, A.M., Frank, J.S., Demer, L.L., Edwards, P.A., Watson, A.D., Lusis, A.J., 1995. Atherosclerosis: basic mechanisms: oxidation, inflammation, and genetics. Circulation 91, 2488–2496.

Berman, J.P., Farkouh, M.E., Rosenson, R.S., 2013. Emerging anti-inflammatory drugs for atherosclerosis. Expert Opin. Emerg. Drugs 18, 193–205.

Carstens, M.G., Bevernage, J.J.L., van Nostrum, C.F., van Steenbergen, M.J., Flesch, F.M., Verrijk, R., de Leede, L.G.J., Crommelin, D.J.A., Hennink, W.E., 2007. Small oligomeric micelles based on end group modified mPEG-oligocaprolactone with monodisperse hydrophobic blocks. Macromolecules 40, 116–122.

Carstens, M.G., van Nostrum, C.F., Verrijk, R., de Leede, L.G., Crommelin, D.J., Hennink, W.E., 2008. A mechanistic study on the chemical and enzymatic degradation of PEG-Oligo(ε-caprolactone) micelles. J. Pharm. Sci. 97, 506–518.

Chowdhary, R.K., Sharif, I., Chansarkar, N., Dolphin, D., Ratkay, L., Delaney, S., Meadows, H., 2003. Correlation of photosensitizer delivery to lipoproteins and efficacy in tumor and arthritis mouse models; comparison of lipid-based and Pluronic P123 formulations. J. Pharm. Pharm. Sci. 6, 198–204.

Cramers, P., Ruevekamp, M., Oppelaar, H., Dalesio, O., Baas, P., Stewart, F.A., 2003. Foscan® uptake and tissue distribution in relation to photodynamic efficacy. Br. J. Cancer 88, 283–290.

Davidsen, M., Brønnum-Hansen, H., Jørgensen, T., Madsen, M., Gerdes, L.U., Osler, M., Schroll, M., 2002. Trends in incidence, case-fatality and recurrence of myocardial infarction in the Danish MONICA population 1982–1991. Eur. J. Epidemiol. 17, 1139–1145.

Demidova, T., Hamblin, M., 2004. Macrophage-targeted photodynamic therapy. Int. J. Immunopathol. Pharmacol. 17, 117–126.

Drakopoulou, M., Toutouzas, K., Michelongona, A., Tousoulis, D., Stefanadis, C., 2011. Vulnerable plaque and inflammation: potential clinical strategies. Curr. Pharm. Des. 17, 4190–4209.

Fang, J., Nakamura, H., Maeda, H., 2011. The EPR effect: unique features of tumor blood vessels for drug delivery, factors involved, and limitations and augmentation of the effect. Adv. Drug Deliv. Rev. 63, 136–151.

Farb, A., Sangiorgi, G., Carter, A.J., Walley, V.M., Edwards, W.D., Schwartz, R.S., Virmani, R., 1999. Pathology of acute and chronic coronary stenting in humans. Circulation 99, 44–52.

Gotto, A.M., Pownall, H.J., 2015. Prevention and treatment of atherosclerotic vascular disease: hypolipidemic agents. In: Jagadeesh, G., Balakumar, P., Maung-U, K. (Eds.), Pathophysiology and Pharmacotherapy of Cardiovascular Disease. Springer International Publishing AG, Switzerland, pp. 589–611.

Gray, B.H., Sullivan, T., 1996. The treatment of iliac artery atherosclerosis with angioplasty and intravascular stents. Vasc. Med. 1, 287–291.

Guo, H., Qian, H., Idris, N.M., Zhang, Y., 2010. Singlet oxygen-induced apoptosis of cancer cells using upconversion fluorescent nanoparticles as a carrier of photosensitizer. Nanomedicine: NBM 6, 486–495.

Henderson, B.W., Dougherty, T.J., 1992. How does photodynamic therapy work? Photochem. Photobiol. 55, 145–157.

Hofman, J.W., Carstens, M.G., van Zeeland, F., Helwig, C., Flesch, F.M., Hennink, W.E., van Nostrum, C.F., 2008. Photocytotoxicity of mTHPC (temoporfin) loaded polymeric micelles mediated by lipase catalyzed degradation. Pharm. Res. 25, 2065–2073.

Jenkins, M.P., Buonaccorsi, G.A., Raphael, M., Nyamekye, I., McEwan, J.R., Bown, S.G., Bishop, C.C., 1999. Clinical study of adjuvant photodynamic therapy to reduce restenosis following femoral angioplasty. Br J Surg 86, 1258–1263.

John, H., Kitas, G., 2012. Inflammatory arthritis as a novel risk factor for cardiovascular disease. Eur. J. Intern. Med. 23, 575–579.

Jori, G., Reddi, E., 1993. The role of lipoproteins in the delivery of tumour-targeting photosensitizers. Int. J. Biochem. 25, 1369–1375.

Kachatkou, D., Sasnouski, S., Zorin, V., Zorina, T., D'Hallewin, M.A., Guillemin, F., Bezdetnaya, L., 2009. Unusual photoinduced response of mTHPC liposomal formulation (Foslip). Photochem. Photobiol. 85, 719–724.

Konan, Y.N., Gurny, R., Allemann, E., 2002. State of the art in the delivery of photosensitizers for photodynamic therapy. J. Photochem. Photobiol. B 66, 89–106.

Kuznetsova, N., Makarova, E., Dashkevich, S., Gretsova, N., Kalmykova, E., Negrimovsky, V., Kaliya, O.L., Lukyanets, E.A., 2000. Structure-photochemical properties relationship for porphyrins and related compounds. Zh. Obshch. Khim. 70, 140–148.

Libby, P., Ridker, P.M., Maseri, A., 2002. Inflammation and atherosclerosis. Circulation 105, 1135–1143.

Lobatto, M.E., Calcagno, C., Millon, A., Senders, M.L., Fay, F., Robson, P.M., Ramachandran, S., Binderup, T., Paridaans, M.P., Sensarn, S., Rogalla, S., Gordon, R.E., Cardoso, L., Storm, G., Metselaar, J.M., Contag, C.H., Stroes, E.S., Fayad, Z.A., Mulder, W.J., 2015. Atherosclerotic plaque targeting mechanism of long-circulating nanoparticles established by multimodal imaging. ACS Nano 9, 1837–1847.

Lorenz, K., Maier, H., 2008. Plattenepithelkarzinome im Kopf-Hals-Bereich. HNO 56, 402–409.

Ma, J., Chen, J.Y., Idowu, M., Nyokong, T., 2008. Generation of singlet oxygen via the composites of water-soluble thiol-capped cdte quantum dots sulfonated aluminum phthalocyanines. J. Phys. Chem. B 112, 4465–4469.

Makhseed, S., Tuhl, A., Samuel, J., Zimcik, P., Al-Awadi, N., Novakova, V., 2012. New highly soluble phenoxy-substituted phthalocyanine and azaphthalocyanine derivatives: synthesis, photochemical and photophysical studies and atypical aggregation behavior. Dyes Pigments 95, 351–357.

Michael-Titus, A.T., Whelpton, R., Yaqub, Z., 1995. Binding of temoporfin to the lipoprotein fractions of human serum. Br. J. Clin. Pharmacol. 40, 594–597.

Mulder, W.J., Jaffer, F.A., Fayad, Z.A., Nahrendorf, M., 2014. Imaging and nanomedicine in inflammatory atherosclerosis. Sci. Transl. Med. 6 (239sr1).

Nombona, N., Maduray, K., Antunes, E., Karsten, A., Nyokong, T., 2012. Synthesis of phthalocyanine conjugates with gold nanoparticles and liposomes for photodynamic therapy. J. Photochem. Photobiol. B: Biol. 107, 35–44.

O'Brien, K.D., Gordon, D., Deeb, S., Ferguson, M., Chait, A., 1992. Lipoprotein lipase is synthesized by macrophage-derived foam cells in human coronary atherosclerotic plaques. J. Clin. Invest. 89, 1544–1550.

Ozoemena, K., Kuznetsova, N., Nyokong, T., 2001. Photosensitized transformation of 4-chlorophenol in the presence of aggregated and non-aggregated metallophthalocyanines. J. Photochem. Photobiol. A Chem. 139, 217–224.

Polo, L., Valduga, G., Jori, G., Reddi, E., 2002. Low-density lipoprotein receptors in the uptake of tumour photosensitizers by human and rat transformed fibroblasts. Int. J. Biochem. Cell Biol. 34, 10–23.

Reshetov, V., Kachatkou, D., Shmigol, T., Zorin, V., D'Hallewin, M.A., Guillemin, F., Bezdetnaya, L., 2011. Redistribution of meta-tetra(hydroxyphenyl)chlorin (m-THPC) from conventional and PEGylated liposomes to biological substrates. Photochem. Photobiol. Sci. 10, 911–919.

Reshetov, V., Zorin, V., Siupa, A., D'Hallewin, M.A., Guillemin, F., Bezdetnaya, L., 2012. Interaction of liposomal formulations of meta-tetra(hydroxyphenyl)chlorin (temoporfin) with serum proteins: protein binding and liposome destruction. Photochem. Photobiol. 88, 1256–1264.

Roger, V.L., Go, A.S., Lloyd-Jones, D.M., Benjamin, E.J., Berry, J.D., Borden, W.B., Bravata, D.M., Dai, S., Ford, E.S., Fox, C.S., Fullerton, H.J., Gillespie, C., Hailpern, S.M., Heit, J.A., Howard, V.J., Kissela, B.M., Kittner, S.J., Lackland, D.T., Lichtman, J.H., Lisabeth, L.D., Makuc, D.M., Marcus, G.M., Marelli, A., Matchar, D.B., Moy, C.S., Mozaffarian, D., Mussolino, M.E., Nichol, G., Paynter, N.P., Soliman, E.Z., Sorlie, P.D., Sotoodehnia, N., Turan, T.N., Virani, S.S., Wong, N.D., Woo, D., Turner, M.B., 2012. Heart disease and stroke statistics-2012 update: a report from the American Heart Association. Circulation 125, e2–e220.

Sanchez-Gaytan, B.L., Fay, F., Lobatto, M.E., Tang, J., Ouimet, M., Kim, Y., van der Staay, S.E., van Rijs, S.M., Priem, B., Zhang, L., Fisher, E.A., Moore, K.J., Langer, R., Fayad,

Z.A., Mulder, W.J., 2015. HDL-mimetic PLGA nanoparticle to target atherosclerosis plaque macrophages. Bioconjug. Chem. 26, 443–451.
Sarjeant, J.M., Rabinovitch, M., 2002. Understanding and treating vein graft atherosclerosis. Cardiovasc. Pathol. 11, 263–271.
Sasnouski, S., Zorin, V., Khludeyev, I., D'Hallewin, M.A., Guillemin, F., Bezdetnaya, L., 2005. Investigation of Foscan interactions with plasma proteins. Biochim. Biophys. Acta 1725, 394–402.
Smolina, K., Wright, F.L., Rayner, M., Goldacre, M.J., 2012. Long-term survival and recurrence after acute myocardial infarction in England, 2004 to 2010. Circ. Cardiovasc. Qual. Outcomes 5, 532–540.
Song, Y., Wennink, J.W., Kamphuis, M.M., Sterk, L.M., Vermes, I., Poot, A.A., Feijen, J., Grijpma, D.W., 2011a. Dynamic culturing of smooth muscle cells in tubular poly (trimethylene carbonate) scaffolds for vascular tissue engineering. Tissue Eng. A 17, 381–387.
Song, Y., Wennink, J.W., Poot, A.A., Vermes, I., Feijen, J., Grijpma, D.W., 2011b. Evaluation of tubular poly(trimethylene carbonate) tissue engineering scaffolds in a circulating pulsatile flow system. Int. J. Artif. Organs 34, 161–171.
Svensson, J., Johansson, A., Grafe, S., Gitter, B., Trebst, T., Bendsoe, N., Andersson-Engels, S., Svanberg, K., 2007. Tumor selectivity at short times following systemic administration of a liposomal temoporfin formulation in a murine tumor model. Photochem. Photobiol. 83, 1211–1219.
Szelenyi, I., 2012. Nanomedicine: evolutionary and revolutionary developments in the treatment of certain inflammatory diseases. Inflamm. Res. 61, 1–9.
Tabas, I., Glass, C.K., 2013. Anti-inflammatory therapy in chronic disease: challenges and opportunities. Science 339, 166–172.
Talelli, M., Barz, M., Rijcken, C.J., Kiessling, F., Hennink, W.E., Lammers, T., 2015. Core-crosslinked polymeric micelles: principles, preparation, biomedical applications and clinical translation. Nano Today 10, 93–117.
Tanielian, C., Schweitzer, C., Mechin, R., Wolff, C., 2001. Quantum yield of singlet oxygen production by monomeric and aggregated forms of hematoporphyrin derivative. Free Radic. Biol. Med. 30, 208–212.
van der Valk, F.M., van Wijk, D.F., Lobatto, M.E., Verberne, H.J., Storm, G., Willems, M.C., Legemate, D.A., Nederveen, A.J., Calcagno, C., Mani, V., Ramachandran, S., Paridaans, M.P., Otten, M.J., Dallinga-Thie, G.M., Fayad, Z.A., Nieuwdorp, M., Schulte, D.M., Metselaar, J.M., Mulder, W.J., Stroes, E.S., 2015. Prednisolone-containing liposomes accumulate in human atherosclerotic macrophages upon intravenous administration. Nanomedicine: NBM 11, 1039–1046.
Van Nostrum, C.F., 2011. Covalently cross-linked amphiphilic block copolymer micelles. Soft Matter 7, 3246–3259.
Waksman, R., McEwan, P.E., Moore, T.I., Pakala, R., Kolodgie, F.D., Hellinga, D.G., Seabron, R.C., Rychnovsky, S.J., Vasek, J., Scott, R.W., Virmani, R., 2008. PhotoPoint photodynamic therapy promotes stabilization of atherosclerotic plaques and inhibits plaque progression. J. Am. Coll. Cardiol. 52, 1024–1032.
Zhu, T.C., Liu, B., Kim, M.M., McMillan, D., Liang, X., Finlay, J.C., Busch, T.M., 2014. Comparison of singlet oxygen threshold dose for PDT. Proc. SPIE Int. Soc. Opt. Eng. 8931, 89310I.